NIH Public Access
Author Manuscript
J Surg Res. Author manuscript; available in PMC 2012 September 1.

Published in final edited form as:
J Surg Res. 2011 September ; 170(1): e179–e188. doi:10.1016/j.jss.2011.05.042.

Aortic Implantation of Mesenchymal Stem Cells after Aneurysm Injury in a Porcine Model

Irene C. Turnbull, MD[a,b], **Lahouaria Hadri, PhD**[b], **Kleopatra Rapti, PhD**[b], **Mikel Sadek, MD**[c], **Lifan Liang, MD**[b], **Hyun J. Shin, MD**[a], **Kevin D. Costa, PhD**[b], **Michael L. Marin, MD**[a], **Roger J. Hajjar, MD**[b], and **Peter L. Faries, MD**[a]

[a] Department of Surgery, Division of Vascular Surgery, Mount Sinai School of Medicine, New York, NY

[b] Cardiovascular Research Center, Mount Sinai School of Medicine. New York, NY

[c] Department of Surgery, New York University School of Medicine, New York , NY

Abstract

Background—Cell based therapies are being evaluated in the setting of degenerative pathophysiological conditions. The search for the ideal method of delivery and improvement in cell engraftment continue to pose a challenge. This study explores the feasibility of introducing mesenchymal stem cells (MSC) following aortic injury in a porcine model.

Methods—Bone marrow derived MSC were obtained from 8 pigs, characterized for the MSC markers CD13 and CD 29, labeled with green fluorescent protein (GFP), and collected for autologous injection in a porcine model of abdominal aortic aneurysm (AAA). The pigs were euthanized (1–7 days) after the procedure to assess the histological characteristics and presence of MSC in the aortic tissue. Negative controls included non-injured aorta. Tracking of the MSC was conducted by the identification of the GFP labeled cells using immunofluorescence.

Results—AAA sections stained with hematoxylin and eosin showed disorganization of the aortic tissue; collagen-muscle-elastin stain demonstrated fragmentation of elastin fibers. The presence of the implanted MSC in the aortic wall was evidenced by fluorescent microscopy showing GFP labeled cells. Engraftment of MSC up to 7 days after introduction was observed.

Conclusion—. Autologous implantation of bone marrow derived MSC following aortic injury in a porcine model may be successfully accomplished. The long term impact and therapeutic value of such cell-based therapy will require further investigation.

Keywords

mesenchymal stem cell; abdominal aortic aneurysm; porcine model; aortic injury; cell therapy; cell implantation

© 2011 Elsevier Inc. All rights reserved.

Corresponding Author: Peter L. Faries, MD, FACS, Chief, Division of Vascular Surgery, Mount Sinai School of Medicine, 5 East 98th Street, Box 1273, New York, NY 10029, Telephone: 212 241 5386, Fax: 212 534 4079, peter.faries@mssm.edu.

Publisher's Disclaimer: This is a PDF file of an unedited manuscript that has been accepted for publication. As a service to our customers we are providing this early version of the manuscript. The manuscript will undergo copyediting, typesetting, and review of the resulting proof before it is published in its final citable form. Please note that during the production process errors may be discovered which could affect the content, and all legal disclaimers that apply to the journal pertain.

NIH-PA Author Manuscript
NIH-PA Author Manuscript
NIH-PA Author Manuscript

NIH-PA Author Manuscript

NIH-PA Author Manuscript

NIH-PA Author Manuscript

Introduction

Cell based therapies are currently being evaluated for the treatment of a variety of degenerative pathophysiological conditions. [1–3] Studies in mice suggest that injured cardiovascular tissue partially regenerates through the recruitment of bone marrow derived mesenchymal stem cell (MSC) populations. [4] Furthermore, in a porcine myocardial infarction model, directed stem cell therapy has been effective at repairing damaged cardiovascular tissue and at restoring cardiac function.[5, 6] The degenerative process responsible for aneurysm formation involves a complex pathological remodeling process of the aortic wall, with deregulated synthesis and degradation of structural matrix proteins, particularly elastin and collagen, and depletion of medial smooth muscle cells. This loss of normal integrity of the connective tissue leads to weakening and dilatation of the aortic wall.[7] We hypothesize that MSC may have a potential therapeutic role in reverting the degenerative process resulting in abdominal aortic aneurysm (AAA) formation. However, similar to applications such as cardiomyoplasty, [8] the introduction of a cell based therapy approach for AAA entails a number of challenges, including but not limited to: method of delivery, tracking, survival and engraftment of the cells. Toward this long-term goal, the objective of the present study was to explore the feasibility of implantation of autologous MSC in the aortic wall after injury using a native AAA porcine model.

Material and Methods

Animals

Eight male Yorkshire swine, weighing 25–35 kg were used in this study. All procedures were performed with the approval of the Institutional Animal Care and Use Committee at Mount Sinai School of Medicine, and the animals received humane care in compliance with the Guide for the Care and Use of Laboratory Animals by the Institute of Laboratory Animal Resources, Commission on Life Sciences. [9]

Isolation of MSCs

The animals were sedated, intubated, and maintained under general anesthesia. Bone marrow aspirates from the iliac crest were obtained using an 11-gauge bone marrow biopsy/aspiration needle and collected into a syringe containing EDTA and processed with Ficoll Paque Plus (GE healthcare) for density centrifugation. Isolation of bone marrow derived MSC was performed following established protocols. [5, 10, 11] Briefly, the harvested bone marrow blood sample was mixed with Hanks' Balanced Salt Solution (HBSS) and layered on the Ficoll Paque. After centrifugation (1000 g for 20 minutes), the mononuclear cell layer was recovered from the interface and suspended once in the plasma of the gradient's upper layer, which was then centrifuged at 500 g for 10 minutes. The supernatant was discarded and the cell pellet was suspended in HBSS and centrifuged at 200 g for 10 minutes. Finally, the cell pellet was suspended in medium M199 with Earle's salts and L-glutamine, (Mediatech, Inc.) supplemented with 10% fetal bovine serum. Cells were incubated in 5% CO_2 at 37°C. The culture media was replaced every third day and the cells were subcultured when they reached 80–90% confluence.

Flow cytometry

For phenotypic characterization, expression of MSC markers was performed by flow cytometric analysis using phycoerythrin (PE) conjugated antibodies. Bone marrow derived MSCs from the third passage were analyzed according to protocols specific for each antibody. The cells were incubated with the following antibodies: CD13 (Pharmingen), CD29 (Caltag Lab), CD 45 (Lifespan), CD34 (Caltag Lab), CD 31 (Invitrogen) and the

NIH-PA Author Manuscript

NIH-PA Author Manuscript

NIH-PA Author Manuscript

isotype controls, IgG1-PE (Immunotech), and IgG1-FITC (Invitrogen). Cells were analyzed on the FACS Calibur (BD Biosciences).

Labeling of MSCs

The adenoviral vector (AdGFP) carrying the green fluorescent protein (GFP) under the control of the Cytomegalovirus (CMV) promoter, was produced using the AdEasy Adenoviral vector system. The absence of replication competent virus was verified by PCR for the E1 gene. The viral titer was determined by UV; using the DU Series 700 UV/Vis Scanning Spectrophotometer (Beckman Coulter); OD 260/OD280: 4.7×10^{12}particle/ml. To track the in vivo implanted MSC, the cells were infected after the third passage with AdGFP at multiplicity of infection (MOI) 100. The cells were trypsinized and collected 72 hours after infection and, after centrifugation, the cell pellet was suspended at a concentration of $1x10^{7}$ cells in 1mL of phosphate buffered saline (PBS) for autologous implantation.

Porcine AAA model and MSC implantation

To induce aortic injury, a porcine model of native AAA was used; this model has been described in detail previously. [(12)] Briefly, with the animals under general anesthesia, using a transperitoneal approach, the infrarenal aorta was exposed. The aneurysm was created by first dilating the infrarenal aorta with a 12mm non compliant angioplasty balloon; a solution containing 16000 units of type I collagenase in 10mL of PBS (Worthington Biochemical Corporation) and 1000 units of pancreatic porcine elastase in 110mL of PBS (Sigma-Aldrich) was instilled into the lumen of the dilated segment of the aorta. Transplant of autologous MSCs was performed immediately after the injury. The GFP labeled MSCs were introduced to the injury site by direct injection into the aortic wall as well as injection into the lumen with isolation of the treated aortic segment by cross clamping for 10 minutes.

Aortic tissue procurement

To assess the effect on the aortic wall histology and to detect the presence of the MSCs, the animals were sacrificed at 24 hours (n=2), 72 hours (n=2) and one week (n=4), following the procedure. Prior to euthanasia, computed tomography angiography (CTA) was performed at completion of one week post AAA induction. Euthanasia was achieved by lethal injection of pentobarbital.

The infrarenal aortic segment where MSCs were injected was obtained, as well as suprarenal aortic samples where no injury was performed. The suprarenal segments were used as paired controls for each animal. The aortic tissue samples were preserved for 24 at 4 C in RNAlater (Ambion), which was then removed and the samples were stored at − 80°C for later processing.

Histology

Aortic tissue samples collected at the time of euthanasia were also embedded in optimal cutting temperature medium (OCT Compound, Tissue-Tek) and immediately frozen for histological analysis. Frozen tissue sections (4 micron) were acetone fixed and stained with hematoxylin-eosin (H&E) and collagen-muscle-elastin (CME), a combination of the Masson's Trichrome and Verhoeff stains.

Immunofluorescence

The presence of GFP expressing MSCs was evaluated by immunostaining of frozen tissue sections with rabbit anti-GFP (Invitrogen) as primary antibody, and Texas red goat anti-rabbit IgG (Invitrogen) as secondary antibody. Coverslips were mounted with ProLong Gold antifade reagent with DAPI (Invitrogen). Images were obtained with a Zeiss Axioplan 2 epi-

NIH-PA Author Manuscript

NIH-PA Author Manuscript

NIH-PA Author Manuscript

fluorescence microscope, equipped with a Zeiss AxioCam MRm camera for capturing fluorescent dyes.

Capillary density was assessed by immunofluorescence on cross sections using Von-Willebrand factor (vWF) antibody (DAKO), as endothelial cell marker, and Alexa Fluor 555 donkey anti-Rabbit (Invitrogen) as secondary antibody, with nuclei counterstained with DAPI.

Western blot

Tissue samples were ground using liquid Nitrogen. The powdered tissue was homogenized in RIPA buffer (Tris 50mM, NaCl 150 mM, SDS 0.1 %, Na-Deoxycholate 0.5 %, NP40 1%) using Lysing Matrix D tubes (MP Biochemicals). The protein concentration was determined by the Bradford method using the manufacturer's instructions (BioRad Laboratories). 10ug of each tissue lysate (total protein) were separated by SDS-PAGE electrophoresis. For western blot analysis, proteins were transferred to polyvinylidene fluoride (PVDF) membrane (Millipore) at 300mA for 1h. The blots were blocked in 5% milk in PBS and incubated overnight with rabbit anti-GFP (A11122, Invitrogen) and mouse anti-glyceraldehyde 3-phosphate dehydrogenase antibody (Sigma). Primary antibodies were labeled with horseradish peroxidase (HRP) conjugated secondary antibodies (BioRad). The blot was developed using the chemiluminescence detection system ECL (Millipore).

qRT-PCR analysis

Relative gene expression was determined using two-step quantitative real-time PCR. Total RNA was isolated with TRIzol reagent (Invitrogen) followed by a "clean up" step as described in the RNeasy Isolation kit (Qiagen). Using the High Capacity cDNA Reverse Transcription kit (Applied Biosystems), 1 μg of total RNA was reverse transcribed according to the manufacturer's protocol. Table 1 lists the primers (Sigma) that were used to amplify specific porcine transcripts for MMP9, MMP2 (associated with matrix modulation), IL-1 and TNF (associated with inflammation) based on prior gene microarray studies of this porcine AAA model. [13] Quantitative real-time PCR reactions were performed with Power SYBR Green Master Mix (ABI) on an ABI Prism 7500 Real Time PCR System. The PCR protocol consisted of one cycle at 95 °C (5 min) followed by 40 cycles of 95 °C (15 s), 58°C (15s) and 72 °C (34s). Fold changes in gene expression were determined using the Ct method with normalization to β-actin endogenous control.

qRT-PCR was also performed to determine the local levels of gene expression of vascular endothelial growth factor (VEGF)-A using specific porcine primers, in aortic tissue samples collected 72 hours and one week after MSC injection. Gene fold expression was calculated using suprarenal non-injured segment as control, with normalization to GAPDH endogenous control.

Results

Assessment of aneurysm injury

The successful induction of AAA was confirmed by histological analysis at 1 week post injury (n = 4). CTA in a representative example, showed a >1.5 fold increase in the aortic diameter of the infrarenal segment where the aneurysm injury was induced, compared to the suprarenal aortic segment used as a paired control (Fig. 1A-B). H&E staining of the tissue sections from the injured segment of aorta showed a substantial reduction in the number of cell nuclei in AAA compared to control (Fig. 1C-D), indicating a loss of smooth muscle cells in the tunica media due to aneurysm injury. CME stain showed loss of the normal aortic wall architecture; disruption of the lamellar unit with fraying and straightening of the

NIH-PA Author Manuscript

NIH-PA Author Manuscript

NIH-PA Author Manuscript

elastin fibers, which markedly differed from the normal aortic tissue, that showed elastin fibers in parallel arrangement (Fig. 1E-F). The aortic wall remodeling and inflammation was confirmed in quantitative real-time PCR experiments of aortic tissue one week after AAA; using porcine specific primers, an upregulation of all biomarkers compared to non-injured control was observed: MMP9 (X7.26x10^3), MMP2 (X1.64), IL-1 (X5.92) and TNF- (X1.78) (Fig. 1G).

MSC characterization and labeling

The cells were characterized using CD13 and CD29, both described as mesenchymal stem cell surface markers; CD45 and CD34, hematopoietic lineage markers, and CD31 (PECAM-1) an adhesion molecule expressed on endothelial cells and their bone marrow precursors. [14–16] Flow cytometry analysis demonstrated a pattern consistent with a MSC population, where the percentage of cells positive for CD13 was 58.5% and CD 29 was 99.8%. The percentage of CD45, CD34 and CD31 positive cells, which are expected to be absent in MSCs, was 0.02%, 0.02% and 0.07% respectively (Fig. 2A). Successful infection with Ad-GFP at 72 hours was confirmed by fluorescence microscopy (Fig. 2B-C).

MSC tracking

Western Blot confirmed the presence of GFP in the treated aortic segments at 24 and 72 hours after the injection of MSCs. The suprarenal segments of the same animals that were used as controls, showed no GFP expression, which underscores targeting of the injection site by the MSC delivery technique (Fig. 3A). The implantation of MSCs in the aortic wall was also confirmed by immunofluorescence. Analysis of the aortic segments where the cells were injected reveals MSC-GFP positive cells at 24 hours, 72 hours and one week after cell injection (Fig. 3B-C and Fig. 4). Immunostaining for GFP was negative in the tissue sections of control non-injured aortic segments.

Capillary density

Immunofluorescence with an anti- vWF antibody was used to identify capillaries in the aortic wall. vWF is a glycoprotein produced by endothelial cells and megakaryocytes, it is found in the subendothelial matrix of blood vessels. [17][18] The presence of endothelial cells positive for vWF were detected in the intact endothelium of the suprarenal aortic tissues, while it was largely absent in the areas of destroyed endothelium of the AAA segments (Fig. 5A). In contrast, in the AAA segments, there were a higher density of vWF positive cells forming tubuloluminal structures within the outer layer of the media and through out the adventitia, when compared to suprarenal controls (Fig. 5B).

To further analyze the possible events related to the enhanced capillary density, the local levels of VEGF-A after implantation of MSC were determined using quantitative real-time PCR in aortic tissue samples collected 72 hours and one week after MSC injection. At 72 hours, VEGF-A mRNA expression levels were significantly increased (X3.45 ± 0.06, p=0.003) compared to control non-treated aorta, whereas one week after MSC implantation the expression of VEGF-A mRNA was approximate to control levels (X1.04 ± 0.49) (Fig. 5C).

Discussion

Porcine native AAA model

The first established AAA model was developed in the rat by isolating the abdominal aorta followed by perfusion with elastase. [19] The rat model, as well as subsequent models utilizing elastase and collagenase, was characterized by dilatation of the aortic wall to 1.5 times its native diameter, an inflammatory response at 7 to 10 days and progressive

NIH-PA Author Manuscript

NIH-PA Author Manuscript

NIH-PA Author Manuscript

destruction of the medial elastic fibers. [20], [21] These models, which recapitulate the hallmarks of AAA, have contributed to the understanding of the pathogenesis of aortic aneurysms and the assessment of pharmacologic therapies. [7, 22]

The pig has biomedical importance as a large animal model for human diseases and it is a suitable model in translational research applications by virtue of its physiologic similarities with humans. The AAA porcine model utilized in this study has been previously characterized; a persistent increase in aortic size was observed by magnetic resonance imaging, and histological analysis showed evidence of inflammation and extracellular matrix remodeling, consistent with prior animal models of elastase induced AAA. [12] Subsequent microarray studies performed on the AAA porcine model demonstrated a pattern in gene expression that is consistent with the human disease state and previously described in rodent models.[13] From this prior study, two genes associated with extracellular matrix modulation (MMP2 and MMP9) and two genes associated with inflammation (TNF and IL-1) were chosen for gene profile analysis using qRT-PCR. The genes evaluated in the one week AAA sample were upregulated as expected from prior studies.

Mesenchymal Stem Cells

Multipotent stem cells, unlike pluripotent embryonic stem cells, are adult stem cells with a more restricted potential for differentiation but that still retain the ability of self renewal and the ability to generate progeny of multiple cell lineages. These cells reside within their tissue of origin or in some cases in other tissues that act as stem cell reservoirs, such as the bone marrow. The bone marrow contains two prototypical stem cell populations: the hematopoietic stem cells which give rise to cells of all blood lineages and are able to reconstitute the hematopoietic system; and non-hematopoietic stem cells of the bone marrow stroma that provide the structural and functional support for haemopoiesis and are referred to as MSCs because they can differentiate into multiple cell lineages of mesodermal origin and contribute to the regeneration of mesenchymal tissues such as bone, cartilage, muscle, ligament, tendon, adipose, and stroma. [23] [24] MSCs in the bone marrow differentiate into fibroblasts and osteoblasts. The osteoblasts line the bone surface and support survival of the hematopoietic stem cells, while the fibroblasts may modulate the area where hematopoietic stem cells are recruited to the circulation and proliferate. [25]

Phenotypic characterization of the MSCs includes the use of a variety of cell surface markers. The studies to conduct immunophenotyping for this cell population vary between the source and species. CD 29 and CD 13 have been described as cell surface receptors that characterize bone marrow derived mesenchymal stem cells. CD 45, a well recognized hematopoietic cell marker and CD31, an endothelial cell marker, are used for negative selection of MSCs; CD34, also a hematopoietic lineage marker and endothelial precursor, is not expressed in *in vitro* expanded MSCs. [14] [15] [26][16] The findings from this study correlate with this pattern, as the isolated MSCs presented a higher percentage of cells that were positive for CD29 and CD13 with a very low detection of CD45, CD31 and CD34. The absence of CD45 cells from this population leads to the conclusion that the isolated cells correspond to the stromal component of the bone marrow and not the hematopoietic stem cells.

MSCs have been widely recognized as potential candidates for cell based therapy. It has been described that the homing of these cells to a site of injury can also result in actual MSC-mediated functional repair. [27] MSCs administered by intra-articular injection into the knee joint following injury are capable of specific migration, engraftment and repair of the damaged meniscus and cartilage. [28] Rodent models have provided evidence of the myogenic potential of stem cells. [4, 29] Porcine models of myocardial infarction have further demonstrated the reparative potential of MSCs when administered acutely after injury. [6]

NIH-PA Author Manuscript

NIH-PA Author Manuscript

NIH-PA Author Manuscript

The local injection of MSCs in a porcine model of myocardial infarction not only demonstrated the successful engraftment of locally injected MSCs but also their multi-phenotypic differentiation. These cells evolved into cells that have biologic characteristics of cardiac myocytes and endothelial cells. These findings were described along with improvement of cardiac function when compared with untreated controls. [5]

Potential role of cell therapy in AAA

In the setting of AAA, the capacity of the MSCs to differentiate into cells of the connective tissue lineage is of great interest. The goal of this study was to establish a model that introduces the concept of cell based therapy in AAA. Towards this aim, we demonstrated the successful isolation, expansion, labeling and implantation of the MSCs in the aortic wall.

MSCs enhance wound healing through paracrine factors, such as VEGF, which has chemoattractant and angiogenic properties. Rat bone marrow stromal cells have been reported to induce angiogenic effects through VEGF. MSCs secrete a variety of angiogenic factors, *in vitro* studies have demonstrated increased expression levels of VEGF-A under hypoxia conditions; following these findings, *in vivo studies* showed increased capillary formation in a mouse model of hind limb ischemia, with this effect lasting even after MSC survival was not detectable. [30] A variety of factors play a role in the angiogenic effect of MSCs, it has been shown that VEGF production is enhanced by implanted MSCs, they can also transdifferentiate and adopt immunophenotypic characteristics of endothelial cells, in addition, MSCs also stimulate an angiogenic response through paracrine factors. (31)

VEGF is a regulator of angiogenesis and it also stimulates elastolytic proteinases. Both processes play a role in the pathogenesis of abdominal aortic aneurysms, and therefore an association between the expression of VEGF and the establishment of abdominal aortic aneurysms has been suggested. [32][33] The effects of VEGF are not only related to angiogenesis, inducing migration and proliferation of endothelial cells, but it also has an effect on other types of cells, such as smooth muscle cells, monocytes and macrophages. VEGF upregulates the expression of matrix metalloproteinases in endothelial cells and smooth muscle cells. [32] In the evaluation of atherosclerotic lesions of human aorta, an association between neovascularization and inflammation has been described, and it is suggested that they synergistically play a role in disease progression. [34] Likewise, in the evolution of AAA, angiogenic, immuno-inflammatory and fibrotic responses are observed in the adventitia.[35]

We observed that VEGF-A was overexpressed in the AAA tissue samples at 72 hours, the level of expression reached values similar to control samples at one week. The transient effect of VEGF-A has been recently described, [33] however, it is not clear what are the mechanisms involved. The increased capillary density in AAA tissue sections along with the increased expression of VEGF-A are both characteristics expected to be found in AAA, which further demonstrates the successful creation of AAA, but they are also a feature that can potentially be attributed to the paracrine effect of the engrafted MSCs. Further study is required to determine the long term outcome of this effect.

In the course of this study, we encountered several challenges, such as the short term duration of the expression of GFP that is sustained by the Ad gene transfer. In order to address this caveat and to extend the duration of expression, future studies will include lentiviral vectors. These alternative methods of MSC labeling will improve the process of tracking their presence in the aortic wall for extended time, and allow evaluating their long term effect. The transplantation of MSC immediately following the aneurysmal injury, is not a realistic approach for a clinical scenario, therefore, sequential treatment, with multiple

NIH-PA Author Manuscript

NIH-PA Author Manuscript

NIH-PA Author Manuscript

survival surgeries, for the induction of the aneurysm, and at a later time point, for the administration of the cell-based therapy, will be required.

The regenerative capability of the MSC in the injured aortic tissue remains to be elucidated. Their reparative potential is not straightforward and requires investigation. While the low immunogenic effect of mesenchymal stem cells makes them extensively suitable for many cell based therapy applications, the angiogenesis effect associated with mesenchymal stem cell therapy has been a matter of concern, and a possible association towards tumorigenesis [(36)]. The high potential of MSC to differentiate into cells with a muscular phenotype in a mouse model of femoral arterial injury, has exposed additional challenges; as they proliferated and differentiated into both smooth muscle cells and endothelial-like cells, their presence appeared to contribute to excessive repair processes and was considered a possible source of intimal hyperplasia. [(37)] The need for genetic reprogramming of cells before their delivery is an alternative that could enhance the desired reparative effects of the MSC on the aortic wall. [(38)]

Conclusion

The recent development of the porcine model of native AAA provides a basis to perform studies to evaluate potential cell-based therapies in a pre-clinical animal model that will facilitate future translational application of the results. The successful delivery of autologous bone marrow derived MSCs to the acutely injured aortic wall described in this report is the first step for the development of further in vivo experiments to test the potential contribution of the MSC in the repair and regeneration of the aneurysmal aortic wall.

Acknowledgments

This work was supported by the American Vascular Association William J. von Liebig Award in conjunction with National Institutes of Health Grant K08HL073313 (PF) and K01HL1031176-01 (LH). The authors express their gratitude to Dr. Purushothaman K-Raman and Dr. Meerarani Purushothaman for their critical comments and constructive suggestions.

References

1. Picinich SC, Mishra PJ, Glod J, Banerjee D. The therapeutic potential of mesenchymal stem cells. Cell- & tissue-based therapy. Expert Opin Biol Ther. 2007; 7:965–973. [PubMed: 17665987]
2. Charbord P. Bone marrow mesenchymal stem cells: historical overview and concepts. Hum Gene Ther. 2010; 21 :1045–1056. [PubMed: 20565251]
3. Pal R, Gopinath C, Rao NM, Banerjee P, Krishnamoorthy V, Venkataramana NK, Totey S. Functional recovery after transplantation of bone marrow-derived human mesenchymal stromal cells in a rat model of spinal cord injury. Cytotherapy. 2010; 12 :792–806. [PubMed: 20524772]
4. Orlic D, Kajstura J, Chimenti S, Jakoniuk I, Anderson SM, Li B, Pickel J, McKay R, Nadal-Ginard B, Bodine DM, Leri A, Anversa P. Bone marrow cells regenerate infarcted myocardium. Nature. 2001; 410 :701–705. [PubMed: 11287958]
5. Makkar RR, Price MJ, Lill M, Frantzen M, Takizawa K, Kleisli T, Zheng J, Kar S, McClelan R, Miyamota T, Bick-Forrester J, Fishbein MC, Shah PK, Forrester JS, Sharifi B, Chen PS, Qayyum M. Intramyocardial injection of allogenic bone marrow-derived mesenchymal stem cells without immunosuppression preserves cardiac function in a porcine model of myocardial infarction. J Cardiovasc Pharmacol Ther. 2005; 10 :225–233. [PubMed: 16382259]
6. Grogaard HK, Sigurjonsson OE, Brekke M, Klow NE, Landsverk KS, Lyberg T, Eriksen M, Egeland T, Ilebekk A. Cardiac accumulation of bone marrow mononuclear progenitor cells after intracoronary or intravenous injection in pigs subjected to acute myocardial infarction with subsequent reperfusion. Cardiovasc Revasc Med. 2007; 8:21–27. [PubMed: 17293265]

NIH-PA Author Manuscript

NIH-PA Author Manuscript

NIH-PA Author Manuscript

7. Thompson RW, Curci JA, Ennis TL, Mao D, Pagano MB, Pham CT. Pathophysiology of abdominal aortic aneurysms: insights from the elastase-induced model in mice with different genetic backgrounds. Ann N Y Acad Sci. 2006; 1085 :59–73. [PubMed: 17182923]
8. Paul D, Samuel SM, Maulik N. Mesenchymal stem cell: present challenges and prospective cellular cardiomyoplasty approaches for myocardial regeneration. Antioxid Redox Signal. 2009; 11 :1841–1855. [PubMed: 19260767]
9. Bayne K. Revised Guide for the Care and Use of Laboratory Animals available. American Physiological Society. Physiologist. 1996; 39:199, 208–111. [PubMed: 8854724]
10. Seeger FH, Tonn T, Krzossok N, Zeiher AM, Dimmeler S. Cell isolation procedures matter: a comparison of different isolation protocols of bone marrow mononuclear cells used for cell therapy in patients with acute myocardial infarction. Eur Heart J. 2007; 28 :766–772. [PubMed: 17298974]
11. Jaatinen, T.; Laine, J. Curr Protoc Stem Cell Biol. Vol. Chapter 2. 2007. Isolation of mononuclear cells from human cord blood by Ficoll-Paque density gradient; p. 1
12. Hynecek RL, DeRubertis BG, Trocciola SM, Zhang H, Prince MR, Ennis TL, Kent KC, Faries PL. The creation of an infrarenal aneurysm within the native abdominal aorta of swine. Surgery. 2007; 142 :143–149. [PubMed: 17689678]
13. Sadek M, Hynecek RL, Goldenberg S, Kent KC, Marin ML, Faries PL. Gene expression analysis of a porcine native abdominal aortic aneurysm model. Surgery. 2008; 144 :252–258. [PubMed: 18656633]
14. Guo KT, SchAfer R, Paul A, Gerber A, Ziemer G, Wendel HP. A new technique for the isolation and surface immobilization of mesenchymal stem cells from whole bone marrow using high-specific DNA aptamers. Stem Cells. 2006; 24:2220–2231. [PubMed: 16794266]
15. Deans RJ, Moseley AB. Mesenchymal stem cells: biology and potential clinical uses. Exp Hematol. 2000; 28 :875–884. [PubMed: 10989188]
16. Vacanti V, Kong E, Suzuki G, Sato K, Canty JM, Lee T. Phenotypic changes of adult porcine mesenchymal stem cells induced by prolonged passaging in culture. J Cell Physiol. 2005; 205 : 194–201. [PubMed: 15880640]
17. Pusztaszeri MP, Seelentag W, Bosman FT. Immunohistochemical expression of endothelial markers CD31, CD34, von Willebrand factor, and Fli-1 in normal human tissues. J Histochem Cytochem. 2006; 54:385–395. [PubMed: 16234507]
18. Wolf WC, Harley RA, Sluce D, Chao L, Chao J. Localization and expression of tissue kallikrein and kallistatin in human blood vessels. J Histochem Cytochem. 1999; 47 :221–228. [PubMed: 9889257]
19. Anidjar S, Salzmann JL, Gentric D, Lagneau P, Camilleri JP, Michel JB. Elastase-induced experimental aneurysms in rats. Circulation. 1990; 82:973–981. [PubMed: 2144219]
20. Daugherty A, Cassis LA. Mouse models of abdominal aortic aneurysms. Arterioscler Thromb Vasc Biol. 2004; 24 :429–434. [PubMed: 14739119]
21. Colonnello JS, Hance KA, Shames ML, Wyble CW, Ziporin SJ, Leidenfrost JE, Ennis TL, Upchurch GR Jr, Thompson RW. Transient exposure to elastase induces mouse aortic wall smooth muscle cell production of MCP-1 and RANTES during development of experimental aortic aneurysm. J Vasc Surg. 2003; 38 :138–146. [PubMed: 12844103]
22. Wassef M, Upchurch GR Jr, Kuivaniemi H, Thompson RW, Tilson MD 3rd. Challenges and opportunities in abdominal aortic aneurysm research. J Vasc Surg. 2007; 45 :192–198. [PubMed: 17210410]
23. Pittenger MF, Mackay AM, Beck SC, Jaiswal RK, Douglas R, Mosca JD, Moorman MA, Simonetti DW, Craig S, Marshak DR. Multilineage potential of adult human mesenchymal stem cells. Science. 1999; 284 :143–147. [PubMed: 10102814]
24. Caplan AI, Bruder SP. Mesenchymal stem cells: building blocks for molecular medicine in the 21st century. Trends Mol Med. 2001; 7 :259–264. [PubMed: 11378515]
25. Reinders ME, Fibbe WE, Rabelink TJ. Multipotent mesenchymal stromal cell therapy in renal disease and kidney transplantation. Nephrol Dial Transplant. 2010; 25 :17–24. [PubMed: 19861311]

NIH-PA Author Manuscript

NIH-PA Author Manuscript

NIH-PA Author Manuscript

26. McCarty RC, Gronthos S, Zannettino AC, Foster BK, Xian CJ. Characterisation and developmental potential of ovine bone marrow derived mesenchymal stem cells. J Cell Physiol. 2009; 219 :324–333. [PubMed: 19115243]
27. Jain M, Pfister O, Hajjar RJ, Liao R. Mesenchymal stem cells in the infarcted heart. Coron Artery Dis. 2005; 16 :93–97. [PubMed: 15735401]
28. Bruder SP, Jaiswal N, Ricalton NS, Mosca JD, Kraus KH, Kadiyala S. Mesenchymal stem cells in osteobiology and applied bone regeneration. Clin Orthop Relat Res. 1998:S247–256. [PubMed: 9917644]
29. Chen J, Li Y, Katakowski M, Chen X, Wang L, Lu D, Lu M, Gautam SC, Chopp M. Intravenous bone marrow stromal cell therapy reduces apoptosis and promotes endogenous cell proliferation after stroke in female rat. J Neurosci Res. 2003; 73:778–786. [PubMed: 12949903]
30. Hoffmann J, Glassford AJ, Doyle TC, Robbins RC, Schrepfer S, Pelletier MP. Angiogenic effects despite limited cell survival of bone marrow-derived mesenchymal stem cells under ischemia. Thorac Cardiovasc Surg. 2010; 58 :136–142. [PubMed: 20379963]
31. Al-Khaldi A, Eliopoulos N, Martineau D, Lejeune L, Lachapelle K, Galipeau J. Postnatal bone marrow stromal cells elicit a potent VEGF-dependent neoangiogenic response in vivo. Gene Ther. 2003; 10 :621–629. [PubMed: 12692590]
32. Nishibe T, Dardik A, Kondo Y, Kudo F, Muto A, Nishi M, Nishibe M, Shigematsu H. Expression and localization of vascular endothelial growth factor in normal abdominal aorta and abdominal aortic aneurysm. Int Angiol. 2010; 29 :260–265. [PubMed: 20502414]
33. Kaneko H, Anzai T, Takahashi T, Kohno T, Shimoda M, Sasaki A, Shimizu H, Nagai T, Maekawa Y, Yoshimura K, Aoki H, Yoshikawa T, Okada Y, Yozu R, Ogawa S, Fukuda K. Role of vascular endothelial growth factor-A in development of abdominal aortic aneurysm. Cardiovasc Res. 2011
34. Moreno PR, Purushothaman KR, Fuster V, Echeverri D, Truszczynska H, Sharma SK, Badimon JJ, O'Connor WN. Plaque neovascularization is increased in ruptured atherosclerotic lesions of human aorta: implications for plaque vulnerability. Circulation. 2004; 110 :2032–2038. [PubMed: 15451780]
35. Michel JB, Martin-Ventura JL, Egido J, Sakalihasan N, Treska V, Lindholt J, Allaire E, Thorsteinsdottir U, Cockerill G, Swedenborg J. Novel aspects of the pathogenesis of aneurysms of the abdominal aorta in humans. Cardiovasc Res. 2010
36. Kuhn NZ, Tuan RS. Regulation of stemness and stem cell niche of mesenchymal stem cells: implications in tumorigenesis and metastasis. J Cell Physiol. 2010; 222:268–277. [PubMed: 19847802]
37. Wang CH, Cherng WJ, Yang NI, Kuo LT, Hsu CM, Yeh HI, Lan YJ, Yeh CH, Stanford WL. Late-outgrowth endothelial cells attenuate intimal hyperplasia contributed by mesenchymal stem cells after vascular injury. Arterioscler Thromb Vasc Biol. 2008; 28 :54–60. [PubMed: 17991877]
38. Hodgkinson CP, Gomez JA, Mirotsou M, Dzau VJ. Genetic engineering of mesenchymal stem cells and its application in human disease therapy. Hum Gene Ther. 2010; 21 :1513–1526. [PubMed: 20825283]

NIH-PA Author Manuscript
NIH-PA Author Manuscript
NIH-PA Author Manuscript

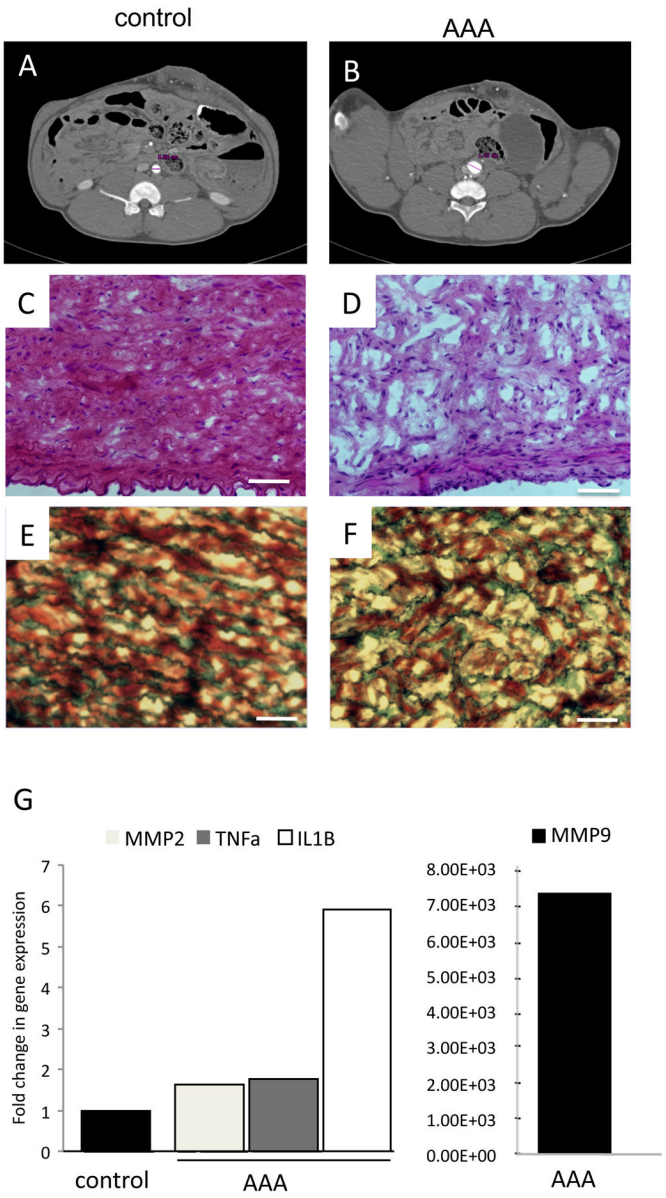

Figure 1. Creation of AAA porcine model

A,B) 1.5 fold increase in aortic diameter at one week after AAA induction (B) demonstrated by CTA, compared to non-injured suprarenal control (A). **C,D)** Photomicrograph of transverse sections of porcine aorta stained with hematoxylin –eosin (H&E) in control (C) and AAA (D). Scale bar= 50μm. **E,F)** Photomicrograph of transverse sections of aorta stained for collagen-muscle–elastin (collagen: green, muscle: red and elastin: black) in control (E) and AAA (F). Scale bar= 50μm. **G)** qRT-PCR: Fold change in gene expression of MMP2, TNFα, IL-1β and MMP9 in AAA aortic tissue compared to non-injured control. MMP9 shown in separate graph with scale that corresponds to the larger fold change.

NIH-PA Author Manuscript
NIH-PA Author Manuscript
NIH-PA Author Manuscript

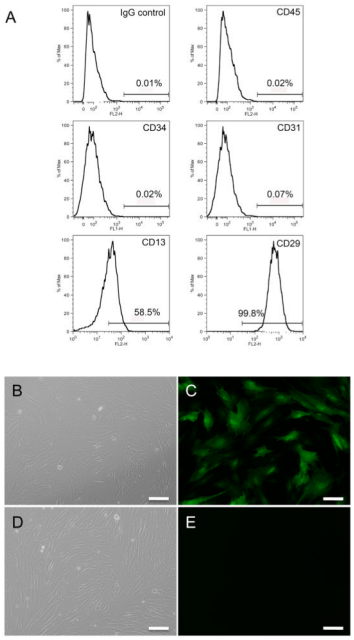

Figure 2. Characterization and Labeling of Porcine Bone Marrow derived MSC

A) Analysis of MSC using flow cytometry: Histogram shows a positive cell population for cell surface markers CD29 and CD13, and negative for CD45, CD34 and CD 31, based on IgG isotype control. **B)** MSC after third passage observed under bright field microscopy. Scale bar=100μm. **C)** Same field of view shows MSC observed under fluorescent microscopy, 72 hours after infection with replication–deficient adenovirus encoding the reporter gene green fluorescent protein (GFP). Scale bar = 100μm. **D)** Non-infected MSC after third passage (control) shown under bright field and **E)** Fluorescence microscopy images obtained using same exposure time in infected and control cells, show absence of GFP positive cells in control.

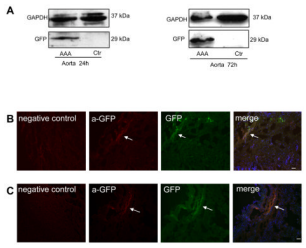

Figure 3. Presence of MSC in aortic wall 24 and 72 hours after injection

A) Western blot analysis of GFP, in the injected infrarenal AAA aortic segment, compared to non-injured suprarenal control at 24h (left panel) and 48h (right panel) after injection of MSC. **B and C)** Successful implantation of MSC demonstrated by immunostaining with anti-GFP at 24h (B) and 48h (C) after MSC injection. Arrow points to site of MSC within the aortic wall in anti-GFP (red), GFP (green), and merge images with DAPI (blue). Control tissues area stained with anti-GFP. Scale bar = 50μm.

NIH-PA Author Manuscript
NIH-PA Author Manuscript
NIH-PA Author Manuscript

NIH-PA Author Manuscript
NIH-PA Author Manuscript
NIH-PA Author Manuscript

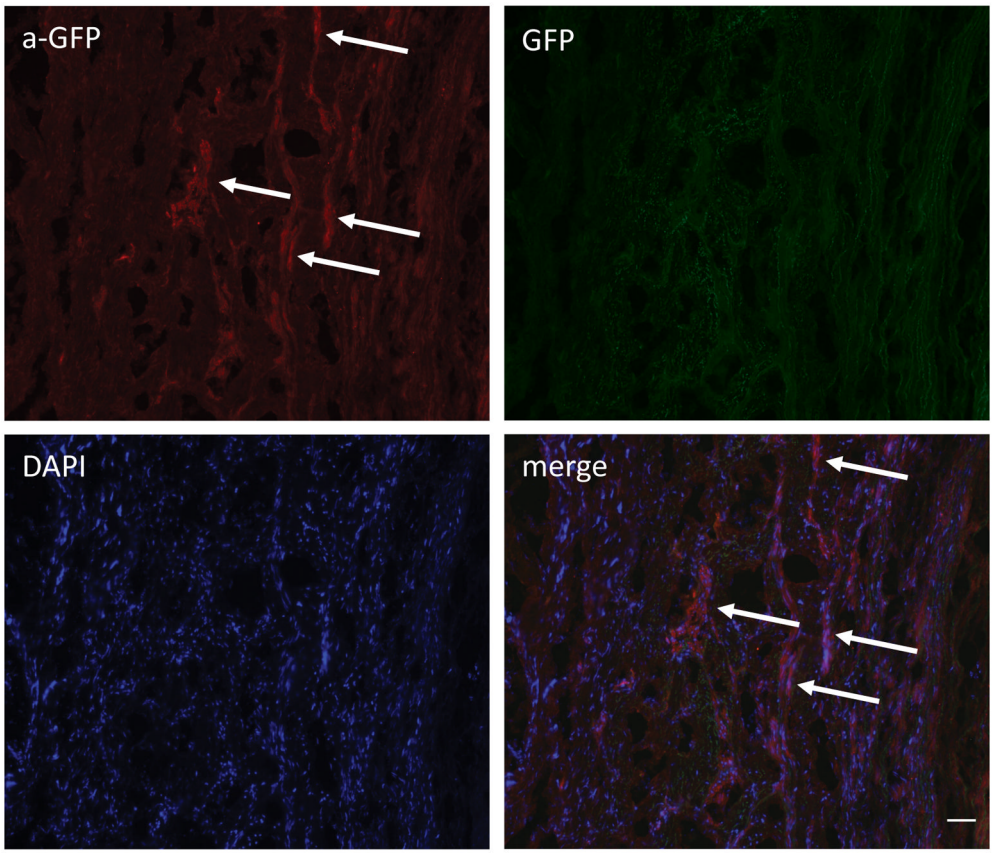

Figure 4. Engraftment of MSC in aortic wall one week after injection

Fluorescent microscopy image with arrows pointing at sites of MSC within the aortic wall labeled with anti-GFP (red). Scale bar = 50μm.

NIH-PA Author Manuscript

NIH-PA Author Manuscript

NIH-PA Author Manuscript

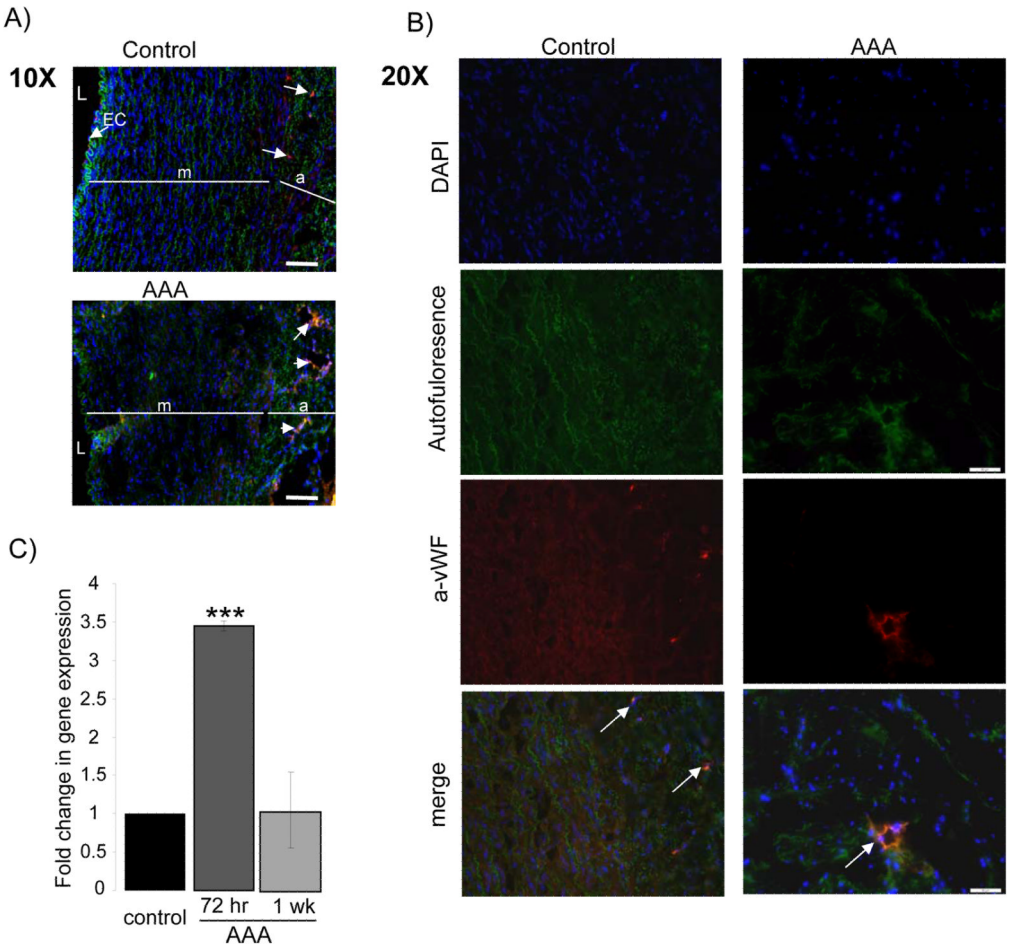

Figure 5.

Identification of capillaries using immunostaining with Von-Willebrand factor antibody (red), nuclei counterstained with DAPI (blue), elastin auto fluorescence (green). **A)** Endothelial cells identified lining the non-injured aortic endothelium in the suprarenal control segment (arrow), these are absent in the injured (AAA) aortic segment. Intact elastin shown in suprarenal control compared to disarranged architecture of the aortic wall in the injured segment with fraying of elastin fibers. L=lumen, EC= endothelial cells, m=media and a=adventitia. Scale bar = 100 μm**B)** Enhanced capillary density was observed in the AAA segment, representative image with arrow pointing to capillary in AAA aortic tissue compared to control. Scale bar = 50 μm. **C)** qRT-PCR: Fold change in gene expression of VEGFA in AAA tissue compared to non-injured control at 72 hours and one week after MSC injection. * Indicates a p-value <.05.

NIH-PA Author Manuscript

NIH-PA Author Manuscript

NIH-PA Author Manuscript

Table 1

Primer sequences used for qRT-PCR analysis.

Gene	Forward Primer	Reverse Primer
MMP9	5’-GGTGGACTATGTGGGCTACG-3’	5’-AGTGCTGAAGCAGGACGAG-3’
MMP2	5’-GCCCCCTTGTCCACTCTTAT-3’	5’-CTTGGTTTTCCTCCATCCAG-3’
IL-1β	5’-CACTGAGCCAGCCTTCTCTC -3’	5’-GACCCTAGTGTGCCATGGTT-3’
TNFα	5’-CCACCACCAAGAATTGGAAC-3’	5’-TTGCATCCAGGAATCCAAAC-3’
β-actin	5’-CTCGATCATGAAGTGCGACGT-3’	5’-GTGATCTCCTTCTGCATCCTGTC-3’
VEGFA	5’-GAGACCCTGGTGGACATCTT-3’	5’-ACACTCCAGACCTTCGTCGT-3’
GAPDH	5’-ACATGGCCTCCAAGGAGTAAGA-3’	5’-GATCGAGTTGGGGCTGTGACT-3’